4892–4905 *Nucleic Acids Research, 2014, Vol. 42, No. 8* *Published online 20 February 2014*
doi:10.1093/nar/gku149

A small RNA controls a protein regulator involved in antibiotic resistance in *Staphylococcus aureus*

Alex Eyraud, Pierre Tattevin, Svetlana Chabelskaya* and Brice Felden*

Université de Rennes I, Inserm U835, Upres EA2311, Biochimie Pharmaceutique, 2 avenue du Prof. Léon Bernard, 35043 Rennes, France

Received September 16, 2013; Revised January 21, 2014; Accepted February 2, 2014

ABSTRACT

The emergence of *Staphylococcus aureus* strains that are resistant to glycopeptides has led to alarming scenarios where serious staphylococcal infections cannot be treated. The bacterium expresses many small regulatory RNAs (sRNAs) that have unknown biological functions for the most part. Here we show that an *S. aureus* sRNA, SprX (alias RsaOR), shapes bacterial resistance to glycopeptides, the invaluable treatments for Methicillin-resistant staphylococcal infections. Modifying SprX expression levels influences Vancomycin and Teicoplanin glycopeptide resistance. Comparative proteomic studies have identified that SprX specifically downregulates stage V sporulation protein G, SpoVG. SpoVG is produced from the *yabJ-spoVG* operon and contributes to *S. aureus* glycopeptide resistance. SprX negatively regulates SpoVG expression by direct antisense pairings at the internal translation initiation signals of the second operon gene, without modifying bicistronic mRNA expression levels or affecting YabJ translation. The SprX and *yabJ-spoVG* mRNA domains involved in the interaction have been identified, highlighting the importance of a CU-rich loop of SprX in the control of SpoVG expression. We have shown that SpoVG might not be the unique SprX target involved in the glycopeptide resistance and demonstrated that the regulation of glycopeptide sensitivity involves the CU-rich domain of SprX. Here we report the case of a sRNA influencing antibiotic resistance of a major human pathogen.

INTRODUCTION

Staphylococcus aureus is a human and animal pathogen that has spectacular adaptive capacities to various antimicrobial agents. *Staphylococcus aureus* rapidly acquires multiple antibiotic resistances, causing a wide spectrum of nosocomial and community-associated infections, and is thus a major worldwide health problem (1). Since the spread of staphylococcal resistance to β-lactams (such as Methicillin), glycopeptide antibiotics have been the most efficient weapons against Gram-positive infections, including the problematic Methicillin-resistant *S. aureus* (MRSA). Vancomycin and Teicoplanin glycopeptide antibiotics have a similar mode of action on cell wall synthesis (2,3). Unlike β-lactams, glycopeptides do not block enzymes involved in cell wall synthesis, but instead sequester the substrates required for peptidoglycan formation. In 1997, the first *S. aureus* with reduced susceptibility to glycopeptides was reported in Japan (1,4). Since then, a number of cases have been reported worldwide, increasing the threat of incurable staphylococcal infections. Three classes of *S. aureus* Vancomycin-resistance have emerged that differ in Vancomycin susceptibilities: high-level Vancomycin-resistant strains, also called VRSA (Minimum Inhibitory Concentration, MIC $\geq$32 μg/ml), Vancomycin-intermediate *S. aureus* (VISA; MIC, 8–16 μg/ml) and heterogeneous Vancomycin-intermediate *S. aureus* (hVISA), which are strains containing subpopulations of Vancomycin-intermediate daughter cells. High level VRSA appeared as a result of a horizontal transfer of Tn*1546* encoding the multiprotein VanA complex from *Enterococcus faecalis* to MRSA clinical isolates (5). Intermediate glycopeptide resistance of *S. aureus* is much more prevalent and currently, the mechanism of such resistance is unknown. It is thought to result from stepwise accumulations of mutations that confer advantage in the face of drug encounters (6,7). One of the most consistent characteristic of *S. aureus* intermediate-resistant strains (hVISA and VISA) is a cell wall thickening, which might reduce the ability of the Vancomycin to diffuse into the division septum, although the mechanisms underlying the assembly of a thicker cell wall are unknown (5–7). Therefore, there is an urgent need to increase our

*To whom correspondence should be addressed. Tel: +33 2 23 23 48 12; Fax: +33 2 23 23 44 56; Email: svetlana.chabelskaia@univ-rennes1.fr
Correspondence may also be addressed to Brice Felden. Tel: +33 2 23 23 48 51; Fax: +33 2 23 23 44 56; Email: bfelden@univ-rennes1.fr

knowledge of the molecular events involved in antibiotic resistance of this serious pathogen, with a necessary focus on the precious glycopeptides used for MRSA infections.

In *S. aureus*, Methicillin and glycopeptide resistance is adjusted by the *yabJ-spoVG* operon, which is in turn controlled by a nucleotide sequence recognized by the alternative sigma B factor (σB) (8,9). The *yabJ-spoVG* mRNA codes for two proteins: YabJ, which has unknown functions; and stage V sporulation protein G (SpoVG). SpoVG was initially identified in *Bacillus subtilis* and thought to be involved in an unknown way in sporulation (10). However, in non-sporulating bacteria, its mode of action and the molecular mechanisms involved are not known even though it was shown recently that SpoVG is a site-specific DNA-binding protein (11). SpoVG (but not YabJ) was shown to be the major regulator of the *yabJ-spoVG* operon (12). This *yabJ-spoVG* operon has been proposed as the σB-dependent secondary regulator (8). In addition to the control of Methicillin and glycopeptide resistance, deletion of the *yabJ-spoVG* operon was shown to alter the expression of extracellular nuclease, lipase and protease expressions (12) as well as affecting capsule formation and the transcriptional control of *cap* and *esxA* (8,13). Micro-arrays performed on *yabJ-spoVG* deletion in the Newman strain showed that *yabJ-spoVG* antagonizes the effects of σB on the expression levels of several proteins (12).

The coordinated expression of pathogenicity determinants is tightly controlled by a complex network of elements, including two component systems, transcription factors, small metabolites and small regulatory RNAs (sRNAs). Recently, bacterial sRNAs were shown to play a major role in a variety of regulatory processes (14). *Staphylococcus aureus* expresses ~250 sRNAs, most of which have unknown biological functions (15–22). sRNAs control gene expression through various mechanisms, generally at the posttranscriptional level by direct pairing with mRNA targets (23). These interactions positively or negatively regulate translation and/or the stability of the mRNAs. Several *S. aureus* sRNAs have been shown to be involved in pathogenicity, e.g. RNAIII, which regulates the expression of numerous virulence factors (16,24–26). RNAIII is produced at the end of the exponential phase and allows for the transition between synthesis of surface-associated proteins and secreted factors (27). Moreover, the sRNAs SprD and Ssr42 have been shown to be involved in *S. aureus* virulence in animal models of infection (28,29).

Herein we report that the recently identified *S. aureus* sRNA SprX (small pathogenicity island RNA X) (20) shapes bacterial resistance to glycopeptide antibiotics and controls the SpoVG expression. In fact, SprX inhibits SpoVG expression through the direct interaction between a C-rich loop of SprX and *spoVG* ribosomal binding site of *yabJ-spoVG* mRNA. This complex prevents ribosomal loading onto *spoVG*, and specifically inhibits translation of the second downstream gene within the *yabJ-spoVG* operon without altering the stability of the *yabJ-spoVG* mRNA.

MATERIALS AND METHODS

Bacterial strains, culture conditions and susceptibility testing

The bacterial strains and plasmids used in this study are listed in Supplementary Table S1. The bacteria were grown at 37°C in Brain–Heart Infusion broth (BHI, Oxoid) or in Tryptic Soy Broth (TSB, Oxoid). When necessary, the media were supplemented with either 10 μg of chloramphenicol or erythromycin for *S. aureus,* or 50 μg ampicillin per ml for *Escherichia coli*. For the spot assays, overnight cultures of the tested strains were diluted to obtain an OD_{600} of 8. From these cultures, seven consecutive 10-fold dilutions were prepared. Three microliters of each dilution was dropped on Muëller–Hinton (MH) or on MH supplemented by 0.75 or 0.85 μg/ml of Teicoplanin or Vancomycin antibiotics, then incubated for 24 h at 37°C. The first dilution corresponds to 10^7 bacteria. For susceptibility testing, plates containing an antibiotic gradient were prepared as described before (9) except that we used BHI agar plate instead of MH agar plate. Teicoplanin susceptibilities were determined by using Etest strips (BioMerieux, France) on MH agar plates according to the manufacturer's instructions.

Plasmid and strain construction

In pCN38-*sprX*, *sprX2* was expressed from its own promoter. The *sprX2* sequence (containing *sprX* sequence, the 207 bp upstream and 258 bp downstream from *sprX*) was amplified from HG001 genomic DNA as a 615-bp fragment using primers listed in Supplementary Table S2. The pCN38-*sprX_mutL3* was produced using the mutagenized oligonucleotides 'mutfor' and 'mutrev' (Supplementary Table S2). The fragments were flanked with *Pst*I and *Eco*RI restriction sites. The polymerase chain reaction (PCR) products were cloned in pCN38 (30).

To inactivate the HG001 (31) *sprX* genes, DNA fragments upstream and downstream of *sprX* were amplified by PCR from genomic DNA by primers listed in Supplementary Table S2. For the *sprX1*, the upstream fragment was 889 bp long and the downstream fragment was 949 bp long; for *sprX2* the upstream was 988 bp long and the downstream was 949 bp long. A second PCR amplification was done by combining these fragments (using primers sprXD1 and sprXD6 for *sprX1*, and primers 2sprXD1 and 2sprXD4 for *sprX2*). These were then cloned using the *PstI-BamHI* sites in the temperature-sensitive plasmid pBT2 (32). To achieve gene disruption in the genome by homologous recombination, the resulting plasmids pBT2Δ*sprX1* and pBT2Δ*sprX2* were transformed into *S. aureus* strain RN4220 and then into *S. aureus* HG001. Mutants were enriched by cultivation at 42°C. Cells from the stationary phase culture were plated on Tryptic Soy Agar (TSA, Oxoid) plates and incubated at 37°C. Colonies were imprinted on plates that were supplemented with 10 μg/ml chloramphenicol. Chloramphenicol-sensitive colonies were tested by PCR for deletion of *sprX1* and *sprX2*. The deletions were confirmed by northern blot assays. The primers used for constructing pBT2Δ*sprX* are shown in Supplementary Table S2. The *S. aureus*

HG001*ΔyabJ-spoVG::erm* mutant was constructed by transducing the *ΔyabJ-spoVG::erm* mutation of strain RN4220 (9) into strain HG001. The deletion of the *yabJ-spoVG* locus was confirmed by PCR, northern blot and western blot analysis.

SpoVG-His_6 expression and antibody preparation

The pSTM33 vector containing SpoVG-His_6 (9) was electroporated into BL21 strain (DE3, Novagen). Cells were grown in Luria Broth (LB, MO BIO) broth to a 600 nm optical density of 0.5, and SpoVG-His_6 expression was induced with 0.3 mM isopropyl-D-thiogalactopyranoside (IPTG, Eurobio). After 3 h, cells were collected by centrifugation and suspended in 30 ml phosphate-buffered saline (pH 7.4) supplemented with a complete ethylenediaminetetraacetic acid (EDTA)-free protease inhibitor cocktail tablet (Roche) and 0.1 mg/ml DNase. The cells were disrupted and the debris separated by centrifugation at 13 000*g* for 10 min. Purification of the His-tagged protein was performed on nickel Sepharose High Performance columns (HisTrap HP; GE Healthcare) using an ÄKTA fast-performance liquid chromatography system. The correct molecular weight of the purified protein was confirmed by sodium dodecyl sulfate-polyacrylamide gel electrophoresis. One milligram of the purified SpoVG-His_6 was used to raise polyclonal mouse antibodies (Eurogentec, Seraing, Belgium).

Protein isolation and western blots

For the total protein extractions, culture pellets corresponding to 2 ml of culture at an OD_{600} of 1 were suspended in 0.2 ml of lysis buffer [10 mM Tris–HCl, pH 7.5, 20 mM NaCl, 1 mM EDTA, 5 mM $MgCl_2$ and complete EDTA-free protease inhibitor cocktail tablet (Roche) containing 0.1 mg/ml lysostaphin]. Following incubation at 37°C for 10 min, Laemmli sample buffer was added (33). Samples were then boiled for 5 min, separated by sodium dodecyl sulphate-polyacrylamide gel electrophoresis and transferred onto a hybond-P PolyVinyliDene Fluoride (PVDF) membrane (Amersham). To visualize SpoVG, antibodies were used at a dilution of 1:5000. The anti-rabbit antibodies were used at a dilution of 1:20 000. Western blots were revealed using the Amersham ECL Plus detection Kit. Signals were visualized using a Typhoon FLA 9500 and quantified using Image-QuantTL 7.0 (GE Healthcare).

Bidimensional gel electrophoresis

Overnight cultures of bacteria were diluted 1:100 in BHI and grown at 37°C to the exponential phase, then the cells were pelleted for 10 min at 4°C (8000*g*). Pellets of 2-ml culture were suspended in the same lysis buffer already described with the addition of 2 UI of DNase amp grade and 2 UI of RNase A. Following incubation at 37°C for 30 min, 1 ml of Tri-Reagent was added, then the samples were sonicated (3×30 s 20% active cycle). Hundred microliters of chloroform was added to each sample and incubated for 5 min at room temperature (RT). Next, 300 µl of ethanol was added and samples were incubated for 3 min at RT and precipitated overnight at −20°C using acetone. The proteins were centrifuged for 15 min at 4°C (4000*g*) and washed with 1 ml of 80% acetone, then pelleted for 5 min at 4°C (4000*g*). The pellets were dried at RT. Duplicate pellets were dissolved in 200 µl of urea 8 M. 2D-DIGE and mass spectrometry identification of proteins of interest were performed by the Cochin Institute (Paris). Spots corresponding to proteins with expression modified between HG001 wt and Δ*sprX* were subjected to in-gel trypsin digestion, peptide extraction and desalting, followed by MALDI-ToF/ToF analysis. Peptides were analyzed using MASCOT and the NCBInr database to identify the selected protein spots. The average ratio of protein levels was calculated using DeCyder 2D software (GE Healthcare) to determine the change in normalized spot volume between HG001 wt and HG001*ΔsprX* samples. The average ratios are shown in Supplementary Table S3, although the statistical analysis was based on the log of the true ratio measurements.

RNA isolation, northern blots, transcription and RNA labeling

Total RNAs were prepared as previously described (20). For SprX, northern blots were performed with 10 µg of total RNA (15). Specific ^{32}P-labeled probes (Supplementary Table S2) were hybridized with ExpressHyb solution (Clontech) for 90 min, washed, exposed and then scanned with a Typhoon FLA 9500 scanner (GE Healthcare). For the northern blots of *yabJ-spoVG* mRNA, 10 µg of total RNAs were separated by 5% polyacrylamide/8M urea gel. The primer pair oSTM29/oSTM30 (Supplementary Table S2) was used to generate α^{32}P-dCTP-labeled *spoVG*-specific probes by PCR labeling. For *in vitro* experiments, RNAs were transcribed from PCR fragments generated from genomic DNA using the primers described in Supplementary Table S2. To produce the template-encoding SprX_mutL3, mutagenized oligonucleotides were used (Supplementary Table S2). RNA was produced by *in vitro* transcription using MEGAscript (Ambion). 5′-RNA γ^{32}P-dATP labeling was performed (34). The RNA was purified by 8% polyacrylamide/8M urea gel, eluted, ethanol precipitated, then stored at −80°C.

RNA structure probing

Structural assays were performed as previously described (34). SprX was prepared by incubating 14 pmol of unlabeled RNA in a buffer (10 mM Tris–HCl, pH 7.5, 60 mM NaCl, 1 mM EDTA) for 10 min at 25°C. The *yabJ-spoVG*$_{167}$ mRNA was prepared by incubating 1 pmol of labeled RNA in the aforementioned buffer. $MgCl_2$ was added to obtain a final concentration of 2.5 mM and this was then incubated for 10 min at 25°C. Preparation for structural analysis of the duplexes between SprX and *yabJ-spoVG*$_{167}$ mRNA was done by incubating 0.2 pmol of labeled RNA with 10 pmol of unlabeled RNA for 15 min at 25°C. Cleavages with S_1 nuclease (0.063 U/µl),V_1 RNase (6.25×10^{-7} U/µl) and 1.25 mM lead acetate were carried out for 10 min at

25°C in the presence of 1 µg of total yeast tRNA. For sequencing, T_1 at 0.038 U/µl and U_2 at 0.0015 U/µl were used. The reactions were precipitated, and the pellets dissolved in loading buffer II (Ambion). The samples were denatured for 10 min at 65°C before separation on 8% polyacrylamide/8M urea gels. Gels were dried and visualized (Typhoon FLA 9500).

Toeprint assays

The toeprint assays were performed as previously described (20), but with modifications. Annealing mixtures containing 13 nM of *yabJ-spoVG* mRNA with either 67 nM of labeled Toeprint_spoVG or Toeprint_yabJ primers were incubated with a buffer (20 mM Tris–HCl, pH 7.5, 60 mM NH_4Cl) for 2 min at 90°C followed by 1 min at RT. Renaturation was realized in the presence of 10 mM $MgCl_2$ at 25°C for 20 min. For the assays in the presence of SprX, various concentrations of SprX were added before the purified *E. coli* 70S ribosomes. The ribosomes were reactivated for 15 min at 37°C and diluted in the reaction buffer in the presence of 1 mM $MgCl_2$. 33 nM 70S were added in each assay, incubated for 5 min and the $MgCl_2$ was adjusted to 10 mM. After 5 min, 0.83 µM uncharged $tRNA^{fMet}$ was added and this was incubated for 15 min. cDNAs were synthesized with 4 U of AMV RT (Biolabs) for 15 min. Reactions were ended by the addition of 15 µl of loading buffer II (Ambion). The cDNAs were loaded and separated onto 8% polyacrylamide/8M urea gels. Sequencing ladders were generated with the same 5′-end-labeled primer.

RESULTS

SprX affects *S. aureus* resistance to glycopeptide antibiotics

In a large-scale analysis of *S. aureus* N315 strain, we identified the small RNA SprX (alias RsaOR) (20). The SprX sequence is highly conserved among *S. aureus* strains. *sprX* is present in the majority of sequenced *S. aureus* strains and is encoded by genomes of converting phages. Most strains contain one copy of the *sprX* gene as for N315 (35), but some comprise two copies, as for example HG001 (36), or even three copies of *sprX*, as in the case of strain Newman (37). Its expression has been found to decrease during stationary growth phase and to increase on salt stress (20). To elucidate the functions of SprX, we analyzed the phenotypes of strains with different sRNA expression levels. For this purpose, we used HG001 *agr*+ *S. aureus* strain carrying two copies of *sprX* gene (Supplementary Figure S1A). Alignments of SprX1 and SprX2 showed that the RNA sequences are identical in each, except for 3 nt (Supplementary Figure S1B). We disrupted the two copies of *sprX* in strain HG001 (Δ*sprX*) by homologous recombination, thus abolishing SprX expression (Figure 1A). Overexpression of SprX was achieved using a multicopy plasmid expressing SprX from its endogenous promoter (pCN38-*sprX*, Figure 1A). Among the phenotypes tested of strains possessing different SprX expression levels, we measured their resistance to Teicoplanin, a glycopeptide antibiotic. Using Etest strips, we have detected that the deletion of *sprX* slightly increased the resistance to Teicoplanin (MIC 1.5 µg/ml) compared with parent wt HG001 strain (MIC 1 µg/ml). For a thorough analysis of the effect of SprX on glycopeptide susceptibility, we used a spot Population Analysis Profile assay (spot PAP), which allows rapid, sensitive and reproducible qualitative and quantitative testing of antibiotic resistance that is not limited by $\log_2$ dilutions used in the Etest strips (7). We have tested the effect of SprX on susceptibility to Teicoplanin and Vancomycin, two antibiotics from the glycopeptide family (Figure 1B).

SprX deletion and overexpression had no effect on bacterial growth in MH medium. Interestingly, we observed and reproduced a 2-$\log_{10}$ diminution of colony formation with Teicoplanin and Vancomycin antibiotics for the strain overexpressing SprX when compared with wild-type (wt) strain (Figure 1B). We also observed that the *sprX* deletion strain was slightly more resistant than the wt strain when growing on MH with an increased concentration of antibiotics of 0.85 µg/ml (Figure 1C). Similar results were obtained using gradient plates, demonstrating that the deletion of SprX slightly increases while its overexpression reduces resistance to Teicoplanin (Figure 1D).

To assess if these results are relevant in a clinical isolate, we transformed VISA strain Mu50 (4), which carries a single copy of *sprX* in its genome (35), by both pCN38 and pCN38-*sprX* plasmids (Supplementary Figure S2A). Both, the spot PAP and the gradient plate tests showed that SprX overexpression in strain Mu50 resulted in a decrease in Teicoplanin resistance compared with the strain harboring pCN38 empty plasmid (Supplementary Figure S2B and C). Taken together, these results indicate that SprX could be involved in *S. aureus* resistance to Teicoplanin and Vancomycin. This interesting observation prompted us to identify the SprX target(s) involved in this antibiotic resistance, and to elucidate the mechanism of their regulation by SprX.

SprX reduces the expression of a protein involved in bacterial resistance to numerous antibiotics

To identify SprX targets, we analyzed whether SprX modulates the expression of *S. aureus* proteins. We thus compared the protein profiles of HG001 wt and Δ*sprX* strains by bidimensional gel electrophoresis (2D-DiGE). In total, five proteins were identified as being regulated by SprX (Supplementary Table S3) and all of these were upregulated in the Δ*sprX* strain. Interestingly, mass spectrometry analysis of these proteins identified SpoVG, which is involved in bacterial resistance to Methicillin and glycopeptide antibiotics (9).

To confirm the downregulation of SpoVG expression by SprX, SpoVG protein levels were monitored by western blots using polyclonal antibodies raised against the SpoVG protein (Figure 2A). In agreement with the 2D-DiGE data, we observed an increase of SpoVG protein levels in the Δ*sprX* strain (Figure 2A). Furthermore, the effect of *sprX* inactivation resulting in an increase in SpoVG protein levels was detected at

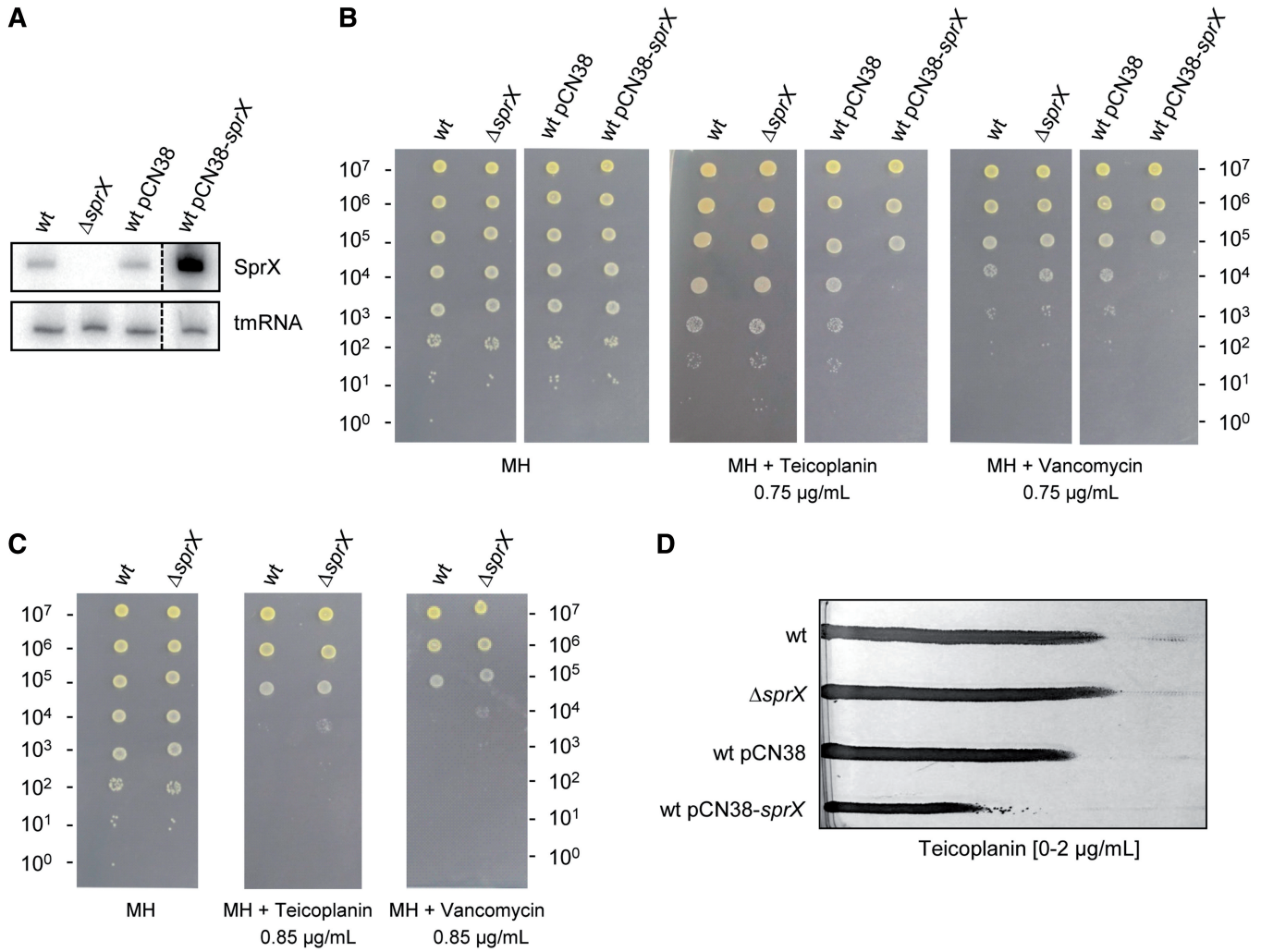

Figure 1. SprX sRNA modulates *S. aureus* resistance to two glycopeptide antibiotics. (**A**) Upper panel: northern blots showing SprX expression when grown until the late-exponential phase in the wt HG001 (wt) strain; HG001Δ*sprX* (Δ*sprX*); wt HG001 transformed by pCN38 (wt pCN38); and wt HG001 transformed by pCN38−*sprX* (wt pCN38-*sprX*). Lower panel: tmRNA used as a loading control. (**B** and **C**) Overnight cultures were prepared in BHI from strains wt HG001 (wt), HG001Δ*sprX* (Δ*sprX*) and wt HG001 transformed by either pCN38 (wt pCN38) or by pCN38-*sprX* (wt pCN38-*sprX*). Ten-fold serial dilutions of cultures were deposited from top (most concentrated: 10^7 bacteria) to bottom (10^0 bacteria) on MH plates and on MH plates supplemented with either Teicoplanin or Vancomycin at 0.75 µg/ml (B) and 0.85 µg/ml (C). They were then incubated for 24 h at 37°C. (**D**) Susceptibility testing of strains from the panel B on gradient plates containing Teicoplanin.

different phases of growth (Supplementary Figure S4). To confirm that the enhanced expression of SpoVG was linked to SprX inactivation, we performed complementation experiments. Introducing pCN38-*sprX* into the Δ*sprX* strain decreased SpoVG protein levels as compared with the Δ*sprX* strain and also compared with those in the wt strain (Figure 2A). These results are explained by the overexpression of SprX from pCN38 compared with its endogenous expression levels in the wt strain. Altogether, these data demonstrate that the SprX sRNA lowers SpoVG expression.

Because SpoVG protein expression is downregulated by SprX, we monitored mRNA levels to determine whether this occurs at transcriptional and/or translational levels. SpoVG is translated from an ∼1200-nt long bicistronic *yabJ-spoVG* mRNA that is cleaved by an unknown mechanism into two transcripts of ∼600 and ∼500 nt, which correspond, respectively, to *yabJ* and *spoVG* mRNAs [(8); Figure 2B]. We used a labeled DNA probe of 300 bp encompassing SpoVG open reading frame (ORF) to detect both the *spoVG* and *yabJ-spoVG* mRNAs (Figure 2B). We also used a labeled DNA probe of 370 bp encompassing the YabJ ORF, which allows the detection of both *yabJ* and *yabJ-spoVG* mRNAs (Supplementary Figure S5A). No significant changes were seen in levels of either mRNA in the Δ*sprX* strain when compared with the wt parental strain (Figure 2C and D and Supplementary Figure S5B and C). Overexpression of SprX did not induce significant changes in the expression levels of full-length *yabJ-spoVG* mRNA, but decreased the amount of both *spoVG* and *yabJ* mRNAs (Figure 2C and D and Supplementary Figure S5B and C). Why the *yabJ* and *spoVG* fragments are produced is currently unknown; however, it has been previously shown that SpoVG is translated from full-length 1200-nt long *yabJ-spoVG* transcript (9). Consequently, our results showing that SprX

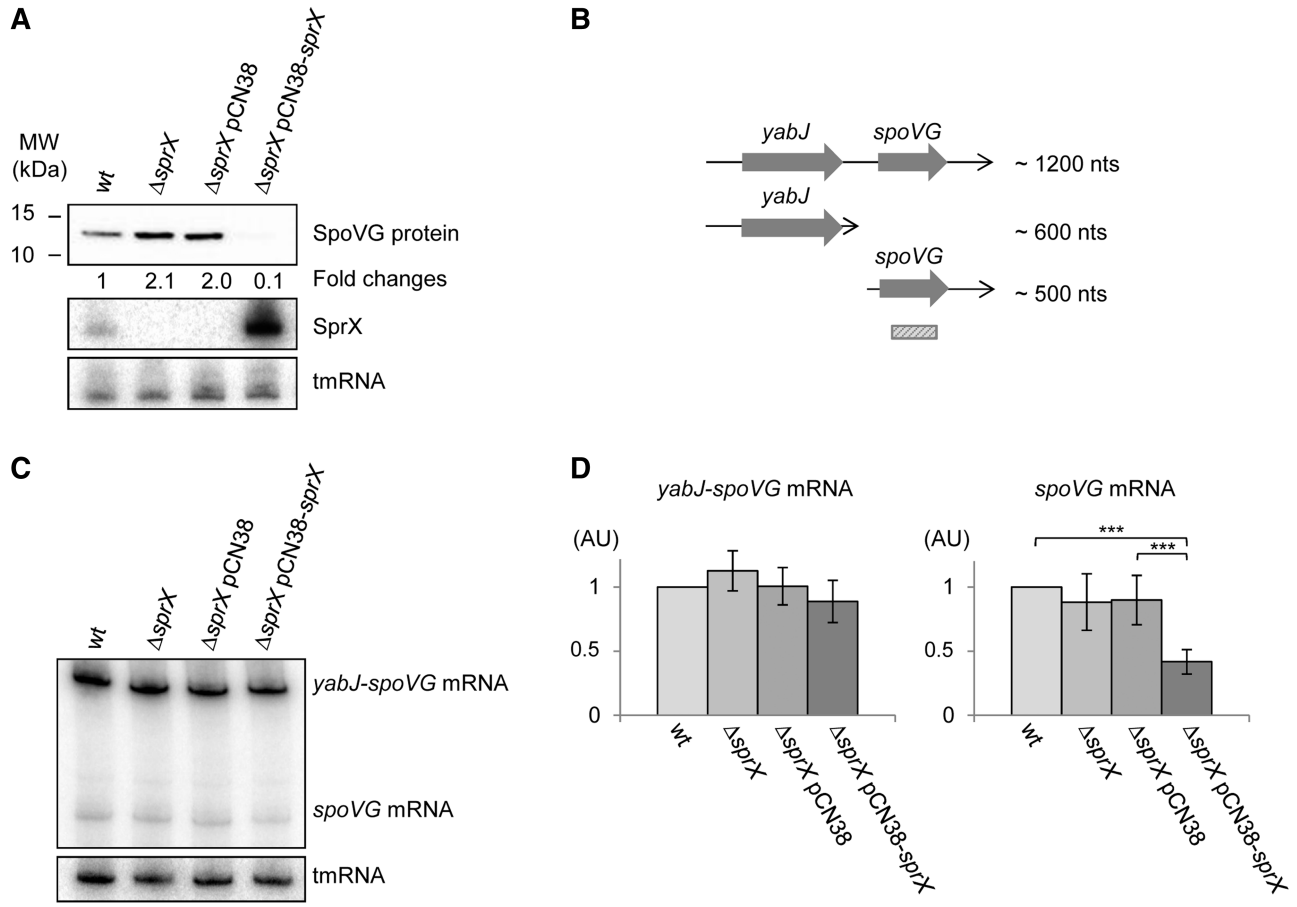

Figure 2. SprX inhibits SpoVG protein expression at the translational level. (**A**) Upper panel: western blot of SpoVG protein levels when grown until the late-exponential phase in the wt HG001 strain (wt), HG001Δ*sprX* (Δ*sprX*) and in HG001Δ*sprX* transformed by either pCN38 (Δ*sprX* pCN38) or pCN38-*sprX* (Δ*sprX* pCN38-*sprX*). Coomassie staining was used as a loading control (Supplementary Figure S3A). SpoVG protein expression levels were calculated relative to the wt strain. The value of the SpoVG protein in wt strain was normalized to 1. Middle panel: northern blots showing SprX expression. Lower panel: tmRNA used as a loading control. (**B**) Schematic representation of *yabJ-spoVG* mRNA. ORFs, mRNA lengths and the probe used for detection by nothern blots of *spoVG* and *yabJ-spoVG* mRNAs are indicated. nts, nucleotides. (**C**) Northern blots detecting the expression levels of *yabJ-spoVG* and *spoVG* mRNAs in wt HG001 strain (wt), HG001Δ*sprX* (Δ*sprX*) and in HG001Δ*sprX* transformed by either pCN38 (Δ*sprX* pCN38) or pCN38-*sprX* (Δ*sprX* pCN38-*sprX*) grown until late-exponential (OD_{600} 9) phases of growth. Probing for the tmRNA was used as a loading control (probes are listed in Supplementary Table S2). (**D**) Northern blot quantification of the levels of *spoVG* and *yabJ-spoVG* mRNAs of the strains from panel C. mRNA expression levels were calculated relative to the value measured for the wt strain. The error bars are the mean values derived from four independent experiments with independent RNA purifications. The tmRNA was used for normalization. The value of the mRNA levels in wild-type strain was normalized to 1. AU, arbitrary units. Difference in expression was measured by student's T-test, $***P < 0.001$.

does not affect the level of *yabJ-spoVG* mRNA suggest that SprX might affect the translation of SpoVG protein.

Structural changes of the *yabJ-spoVG* mRNA induced by SprX

In vivo results prompted us to explore the interaction between SprX and *yabJ-spoVG* mRNA. Interestingly, we identified a putative pairing site between SprX and the translational initiation site of *spoVG in silico* using targetRNA2 (38) and sRNA TarBase (39). The predicted interaction between the two RNAs includes 26 bp and occurs between the U79-U115 nt from SprX and the A566-A606 nt from the *yabJ-spoVG* mRNA [a fragment that includes its Shine–Dalgarno (SD) sequence and the initiation codon of *spoVG*] (Figure 3A). To determine whether SprX interacts with the *yabJ-spoVG* mRNA *in vitro*, we used enzymatic probes to monitor the structural changes of *yabJ-spoVG* mRNA induced by SprX binding. For this purpose, we designed and produced a 167-nt-long mRNA construct, $yabJ\text{-}spoVG_{167}$, which contains the ribosome binding site (RBS) of *spoVG* and the first 86 nt of the *spoVG* ORF (Figure 3B). We subjected the $yabJ\text{-}spoVG_{167}$ alone or in complex with SprX to nuclease S_1 (specific for single-stranded RNAs) and to RNase V_1 cleavages (specific for double-stranded RNAs) (Figure 3C). The presence of many S_1 cleavages in the region A558-A630 of $yabJ\text{-}spoVG_{167}$ mRNA supports the existence of unpaired single-strand domains (Figure 3A and C). These data indicate that the proposed *yabJ-spoVG* mRNA region that binds with SprX is in fact accessible for interaction. SprX-induced structural changes on the $yabJ\text{-}spoVG_{167}$ mRNA are located from A563 to

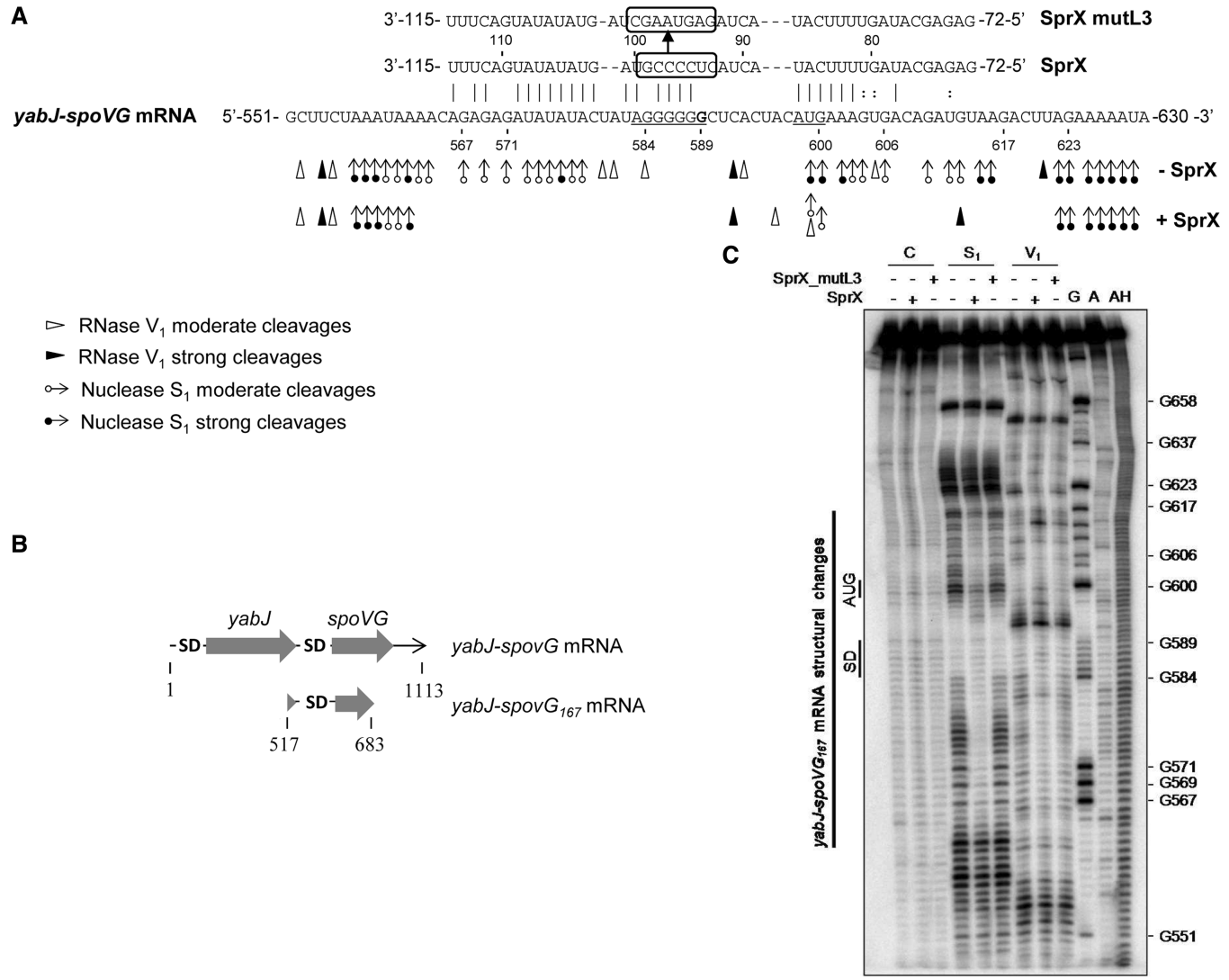

Figure 3. SprX interacts directly with the *yabJ-spoVG* mRNA by base-pairing at the *spoVG* RBS. (**A**) SprX base pairings with the *yabJ-spoVG* mRNA. Binding of SprX encompasses the *spoVG* translational initiation site within the *yabJ-spoVG* mRNA. The SD sequence (5′-AGGGGG-3′) and initiation codon are underlined. The cleavage site of *yabJ-spoVG* mRNA corresponding to G at position 589 (9) is indicated in bold. We outline the mutated nucleotides in SprX_mutL3 for 5′-GAGUAAGC-3′. Probing data in the absence (−SprX) and in the presence of SprX (+SprX) are indicated. Enzymatic cleavages are as follows: moderate (white circle with rightward arrow) and strong (black circle with rightward arrow) S_1 Nuclease cleavages; moderate (white right-pointing pointer) and strong (black right-pointing pointer) RNase V_1 cleavages. (**B**) Schematic representation of *yabJ-spoVG*$_{167}$ mRNA. The two ORFs and the two SD sequences are indicated. (**C**) Structural probing of the *yabJ-spoVG*$_{167}$ mRNA in the presence and absence of SprX. Enzymatic hydrolysis (RNases S_1 and V_1) of 5′-end-labeled *yabJ-spoVG*$_{167}$ mRNA free (−) or with an excess of either SprX or SprX_mutL3. Lanes are as follows: C, control; S_1, nuclease S_1; V_1, RNase V_1; G, RNase T2; A, RNase U2; and AH, alkaline ladder. The bar denotes the localization of the main reactivity changes that are induced by complex formation with SprX but not with SprX_mutL3.

U621 (Figure 3A and C). S_1 cleavages disappeared at positions A563-A578 and A602-A616. Several weak V_1 cleavages situated at A593, U605 and G580-G584 disappeared within the mRNA. Moreover, on duplex formation a strong V_1 cut at position G613 and two weak ones at G596 and U599 appeared in the mRNA. Therefore, we can conclude that the binding of SprX induces structural changes encompassing the SD and AUG initiation codon of *spoVG* in *yabJ-spoVG* mRNA.

We investigated the structure of free SprX (nts 1–150) using chemical and enzymatic probes. To probe the SprX solution structure, we used lead (II) and nuclease S_1, which cleave accessible single-stranded RNA, and RNase V_1, which specifically cleaves double-stranded RNA (Figure 4A). The data support a SprX structure presented in Figure 4B. The simultaneous presence of V_1 and S_1 cleavages at the same nucleotide position within H1-L1 and H2'-L2' may be explained by the coexistence of two alternating structures at the SprX 5′-end (Figure 4B and Supplementary Figure S6). Hairpins H3-L3 and H4-L4 in the 3′ region of SprX are, however, well-supported by the probing patterns. Moreover, a C-rich nucleotide sequence situated within the SprX L3 loop has been proposed to interact through base pairings with the

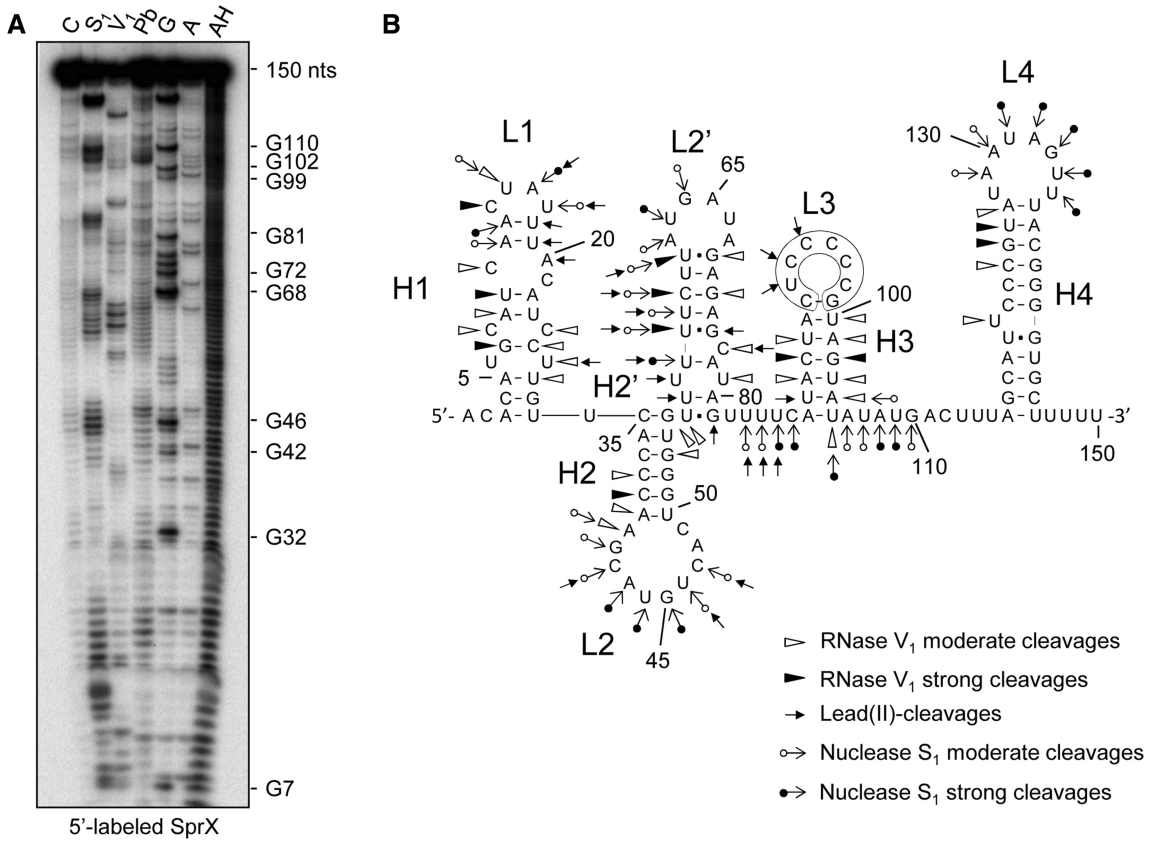

Figure 4. Structural probe monitoring of SprX conformation in solution. (**A**) 5′-labeled SprX was probed by RNase V_1, which cleaves double-strands or stacked nucleotides; and by nuclease S_1 and lead acetate, both of which cleave accessible single-strands. Lanes are as follows: C, control; S_1, Nuclease S_1; V_1, RNase V_1; Pb, lead(II)-induced cleavages; G, RNase T2; A, RNase U2; and AH, alkaline ladder. SprX numbering is on the right. (**B**) Secondary structure of SprX from strain N315 based on probing data. The nucleotide numbering corresponds to SprX2 from HG001 (Supplementary Figure S1). The mutated nucleotides in SprX_mutL3 are outlined on the SprX secondary structure model. Enzymatic cleavages are as follows: moderate (white circle with rightward arrow) and strong (black circle with rightward arrow) S_1 Nuclease cleavages; (rightward arrow) lead(II)-induced cleavages; moderate (white right-pointing pointer) and strong (black right-pointing pointer) RNase V_1 cleavages.

spoVG SD sequence (Figure 3A). We tested the importance of the SprX L3 loop in the interaction between SprX and *yabJ-spoVG* mRNA by mutating the 5′-CUCCCCG-3′ sequence of the SprX L3 loop termed SprX_mutL3 (Figure 3A). The probing pattern of the *yabJ-spoVG* mRNA was identical in the presence of SprX_mutL3 and in the absence of SprX (Figure 3C), implying that the mutated SprX failed to induce structural changes in the *spoVG* RBS of the $yabJ\text{-}spoVG_{167}$ mRNA. These results emphasize the importance of that loop in the interaction with the *yabJ-spoVG* target. Taken together, these mutational data support the proposed model of SprX-*yabJ-spoVG* mRNA interaction (Figure 3A), which involves pairings between the SprX L3 loop and the *spoVG* RBS of the *yabJ-spoVG* mRNA.

SprX specifically reduces *spoVG* translation initiation of the *yabJ-spoVG* operon mRNA

Because SprX interacts with the *spoVG* RBS of *yabJ-spoVG* mRNA covered by the ribosomes during translation initiation, we conjectured that SprX could prevent ribosome loading on the *spoVG* RBS. We tested this hypothesis by performing toeprint analysis. We formed a ternary initiation complex consisting 70S ribosomes, initiator $tRNA^{fMet}$ and *yabJ-spoVG* mRNA. The ribosome blocked the elongation of reverse transcription, and produced a toeprint 16 nt downstream from the AUG initiation codon of *spoVG* (Figure 5A). SprX significantly reduced this toeprint in a concentration-dependent manner, indicating that *in vitro* SprX inhibits ribosome binding onto the *spoVG* RBS of *yabJ-spoVG* mRNA. These results are in agreement with our *in vivo* data, which show that SprX reduces SpoVG protein expression (Figure 2A). Interestingly, SprX_mutL3 failed to prevent ribosome loading onto the *spoVG* of *yabJ-spoVG* mRNA, indicating the essential role of the SprX L3 loop in regulating SpoVG expression (Figure 5A). Because *yabJ-spoVG* is a bicistronic mRNA, we next tested whether SprX might also prevent ribosome loading onto the *yabJ* RBS of the *yabJ-spoVG* mRNA (Figure 5B). One ribosome toeprint was detected 16 nt downstream from the predicted *yabJ* initiation codon. The addition of increasing concentrations of SprX did not alter the ribosome binding. These results show that *in vitro*, SprX specifically inhibits SpoVG translation initiation by antisense pairings with the *spoVG* RBS of the

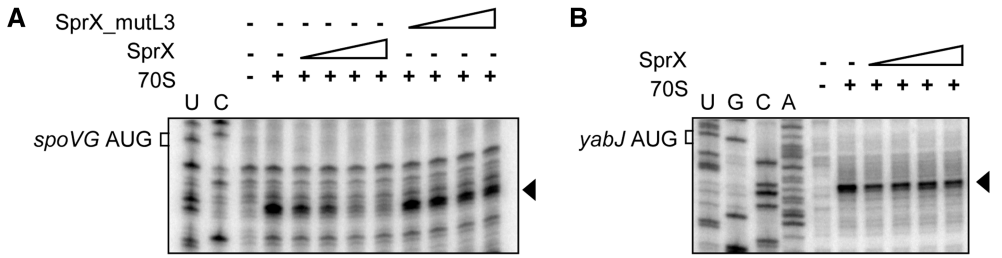

Figure 5. SprX specifically prevents ribosome loading on the *spoVG* translational initiation site within the 1200 nt long *yabJ-spoVG* mRNA. Here we show toeprint assays on (**A**) *spoVG* or (**B**) *yabJ* within the mRNA in the presence of increasing concentrations of SprX or SprX_mutL3 (33, 67, 133 and 267 nM). '+' indicates the presence of purified 70S ribosomes. An arrow indicates the location of the experimentally determined toeprint. U, A, G and C refer to the *yabJ-spoVG* mRNA sequencing ladders.

yabJ-spoVG mRNA, but it has no effect on YabJ translation initiation.

To assess the functional importance of the SprX L3 loop *in vivo*, we tested whether SprX_mutL3 is able to regulate SpoVG protein expression *in vivo*. To address this, we transformed Δ*sprX* strain by pCN38–*sprX_mutL3* and monitored SpoVG protein levels using western blots. Overexpressing SprX strongly reduces SpoVG protein levels (Figure 6). In contrast, overexpressing SprX_mutL3 was unable to inhibit SpoVG protein expression, resulting in SpoVG protein levels identical to those in the strain Δ*sprX* transformed with pCN38 (Figure 6). SprX_mutL3 thus failed to regulate SpoVG expression, demonstrating the importance of the SprX loop in regulating SpoVG *in vivo*. Northern blots indicated that the SprX_mutL3 and wt SprX are expressed at similar levels from pCN38 (Figure 6), indicating that the absence of SpoVG regulation by SprX_mutL3 is not due to its *in vivo* instability. Taken altogether, our *in vitro* and *in vivo* results show that SprX inhibits SpoVG expression at the translational level by antisense pairings occurring between a C-rich loop from SprX and the *spoVG* RBS from *yabJ-spoVG* mRNA.

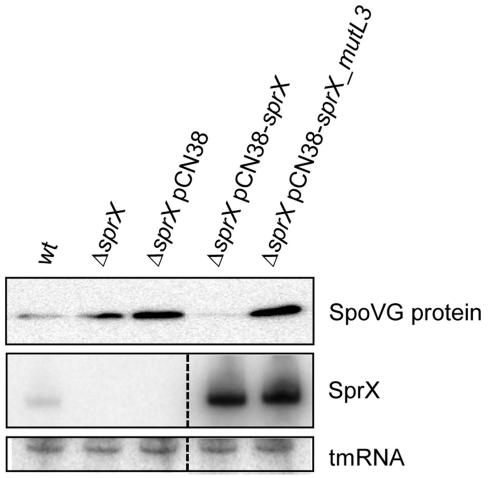

Figure 6. A C-rich loop from SprX is essential in reducing SpoVG expression *in vivo*. Upper panel: western blot analysis of the SpoVG protein levels in wt HG001 strain (wt), HG001Δ*sprX* (Δ*sprX*) and then HG001Δ*sprX* transformed by pCN38 (Δ*sprX* pCN38), pCN38-*sprX* (Δ*sprX* pCN38-*sprX*) or by pCN38-*sprX_mutL3* (Δ*sprX* pCN38-*sprX_mutL3*). Proteins were prepared at the late-exponential phase of growth (OD600 nm of 8). Coomassie staining gel was used as a loading control (Supplementary Figure S3B). Middle panel: northern blot analysis of SprX expression at late-exponential growth phase. Lower panel: tmRNA used as an internal loading control.

SprX influences glycopeptide antibiotic resistance through its C-rich loop

The deletion of the *yabJ-spoVG* operon reduces the resistance to glycopeptide antibiotics in glycopeptide-intermediate-resistant *S. aureus* (9). Complementation by a vector allowing the expression of only the SpoVG protein was sufficient to restore the antibiotic resistance (9). We verified whether the deletion of *yabJ-spoVG* would affect resistance to Teicoplanin and Vancomycin in the susceptible *S. aureus* strain HG001. In agreement with a previous report (9), deletion of the *yabJ-spoVG* operon reduces bacterial resistance to both antibiotics (Figure 7A). To assess if the action of SprX in the *S. aureus* resistance to antibiotics involves other SprX targets in addition to SpoVG, we tested whether SprX is able to modify glycopeptide susceptibility in the absence of SpoVG. For this purpose, we transformed pCN38-*sprX* in strain HG001Δ*yabJ-spoVG*. Overexpression of SprX in this strain slightly reduced bacterial resistance to Teicoplanin and Vancomycin compared with the one transformed with pCN38 (Figure 7B), indicating that, in addition to SpoVG, SprX might control other targets involved in glycopeptide resistance. However, the difference in the Teicoplanin and Vancomycin resistance between HG001Δ*yabJ-spoVG* transformed by pCN38-*sprX* or pCN38 is small, suggesting that the contribution of putative additional SprX targets involved in glycopeptide sensibility is limited compared with SpoVG.

To see if SprX modulates bacterial resistance to glycopeptide antibiotics through its C-rich domain, we tested whether SprX_mutL3 (already shown to not influence SpoVG expression) could affect this susceptibility. We have observed that the effect on antibiotics resistance of *sprX* overexpression is similar to *yabJ-spoVG* deletion (Figures 1B and 7B), and more pronounced than the one observed for *sprX* deletion (Figures 1C and 7B). This could be explained by the moderate effect of *sprX* deletion on SpoVG expression levels (about a 2-fold effect, Figure 2A), while *sprX* overexpression induces a severe decrease in SpoVG expression levels, resembling the *yabJ-spoVG* deletion (~10-fold). However, the strain transformed by pCN38–*sprX_mutL3* exhibits the same

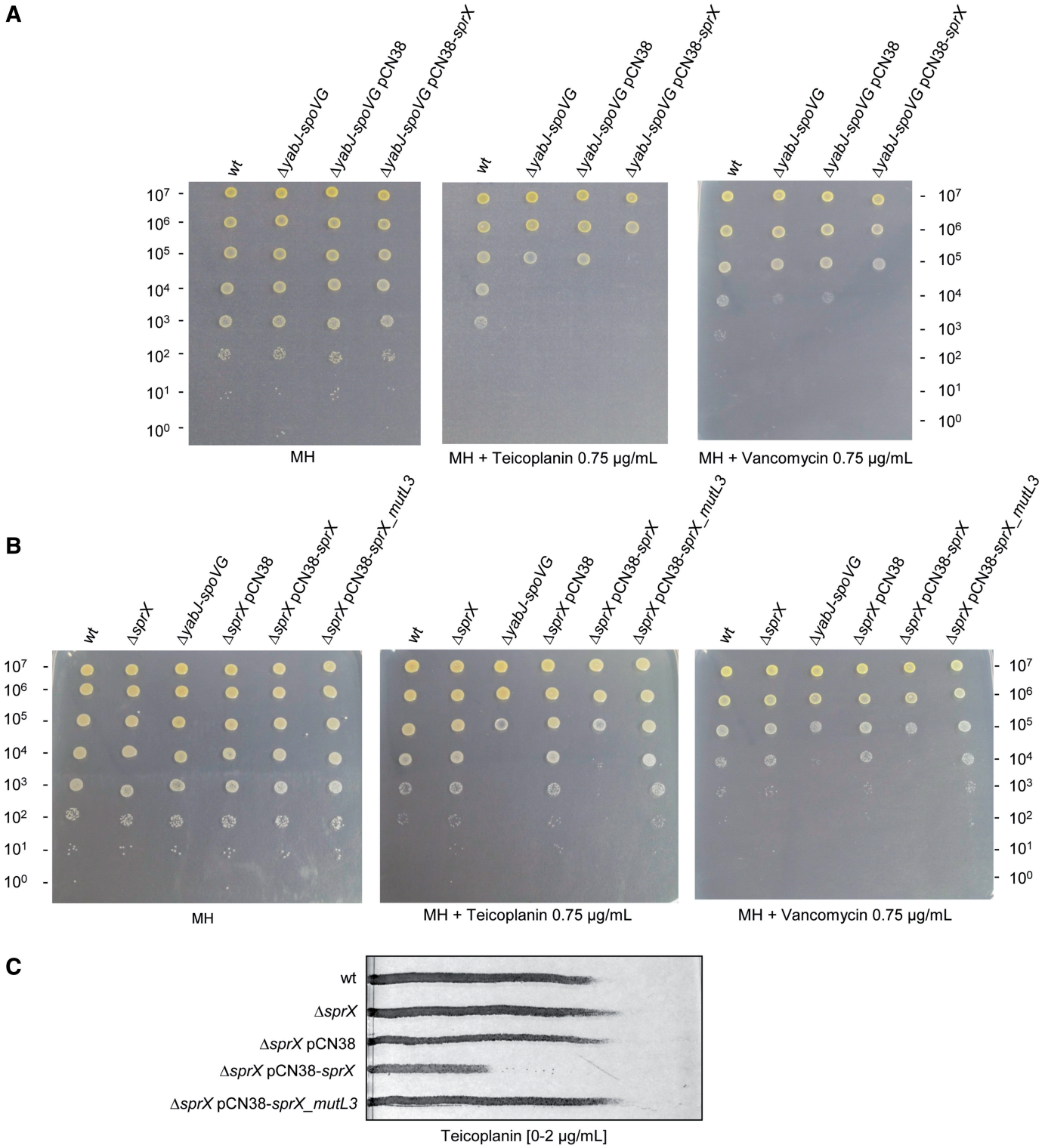

Figure 7. SprX modulates *S. aureus* glycopeptide resistance by its C-rich sequence. (**A**) Ten-fold serial dilutions of overnight cultures were deposited from top (most concentrated: 10^7 bacteria) to bottom (10^0 bacteria) on MH plates or on MH plates supplemented or not with Teicoplanin or Vancomycin (0.75 µg/ml), then incubated at 37°C. Strain are HG001 (wt), HG001Δ*yabJ-spoVG* (Δ*yabJ-spoVG*) and HG001Δ*yabJ-spoVG* transformed by pCN38 (Δ*yabJ-spoVG* pCN38) or pCN38-*sprX* (Δ*yabJ-spoVG* pCN38-*sprX*). (**B**) Ten-fold serial dilutions of strains: wt HG001 strain (wt), HG001Δ*sprX* (Δ*sprX*) and then HG001Δ*sprX* transformed by pCN38 (Δ*sprX* pCN38), pCN38-*sprX* (Δ*sprX* pCN38-*sprX*) or pCN38-*sprX_mutL3* (Δ*sprX* pCN38-*sprX_mutL3*) and HG001Δ*yabJ-spoVG* (Δ*yabJ-spoVG*) were performed and incubated on MH plated supplemented with Teicoplanin or Vancomycin (0.75 µg/ml) at 37°C. (**C**) Level of resistance of strains from panel B on gradient plates containing Teicoplanin.

resistance levels as the one transformed with pCN38 (Figure 7B), indicating that the overexpression of SprX_mutL3 failed to modify their antibiotic susceptibility. Similar results were obtained using gradient plates, illustrating that SprX_mutL3 was unable to modify Teicoplanin resistance (Figure 7C). Collectively, our results emphasize the importance of the C-rich sequence within the third loop of SprX in regulation of SpoVG and the *S. aureus* susceptibility to two glycopeptide antibiotics.

DISCUSSION

Here, we report on the function of SprX (alias RsaOR), a recently identified small RNA expressed from an *S. aureus* pathogenicity island. We provide evidence that SprX shapes *S. aureus* resistance to Vancomycin and Teicoplanin glycopeptides, two invaluable antibiotics for treatment of Methicillin-resistant staphylococcal infections. To investigate the mechanism underlying this modification in antibiotic resistance, we searched for SprX targets. 2D-DiGE analysis of wild-type (wt) and isogenic *sprX* deletion strains allowed us to identify the SpoVG protein, whose expression is reduced by SprX. SpoVG is translated from bicistronic *yabJ-spoVG* mRNA transcribed from a σB-dependent promoter that is responsible for *yabJ-spoVG* mRNA accumulation during bacterial growth (8). The *yabJ-spoVG* operon is involved in capsule formation; controls the expression of extracellular lipase, nuclease and protease; and is also involved in bacterial resistance to Methicillin and glycopeptides (8,9,12).

In fact, SpoVG (not YabJ) is the major regulator of the *yabJ-spoVG* operon (9,12) and on its own it can rescue the phenotypes related to the deletion of the *yabJ-spoVG* operon. However, the molecular mechanisms underlying SpoVG action in these biological pathways remain unknown. Recently, it was reported that SpoVG is a DNA-binding protein supporting the hypothesis that it could act as a transcriptional factor (11). In this report, we found that by reducing SpoVG expression levels, SprX affects *S. aureus* resistance to two glycopeptide antibiotics. Moreover, among other *yabJ-spoVG*–related phenotypes, we tested the effect of SprX on the resistance to Oxacillin and showed that SprX modify the susceptibility to this antibiotic (Supplementary Figure S7). Further studies on the regulation of the additional phenotypes related to *yabJ-spoVG* will be necessary to fully understand the importance of SprX in the regulation of other bacterial processes. We have shown that SpoVG might not be the unique target of SprX involved in the glycopeptide resistance. sRNAs are known to control the expression of multiple mRNA targets, and such mechanism allows a coordinated regulation of factors, involved in joint cellular processes (40).

The effect of SprX overexpression on SpoVG expression and antibiotic susceptibility is more pronounced compared with *sprX* deletion, suggesting that in the wt strain grown under laboratory conditions, SprX could be present in low amounts for the regulation of SpoVG. The effect of *sprX* deletion on SpoVG accumulation is only 2-fold and has a small reproducible effect on antibiotic resistance. Reversely, *sprX* overexpression induces a severe decrease in SpoVG expression (~10 times), which modulates the antibiotic resistance. Because sRNAs are known to allow the bacteria to respond to different environmental changes, some growth conditions could increase SprX expression above the limiting amount to decrease SpoVG expression. On the other hand, the smaller effect of *sprX* deletion compared with overexpression of SprX could be explained by the existence of other SpoVG inhibitors, which could decrease the SpoVG amount in the absence of SprX. Further studies on the control of SprX expression and on other SprX targets will be necessary to fully understand the network of SprX regulation.

We have uncovered the mechanism by which SprX lowers SpoVG expression. SprX interacts by antisense pairings with the *spoVG* ribosomal binding site (including its SD and AUG initiation codon) of the *yabJ-spoVG* mRNA. By mutational analysis, we identified the functional sequence within SprX that interacts with *spoVG* RBS: a C-rich sequence situated in an accessible loop (L3 loop) within the SprX structure. This functional sequence contains an UCCC motif, a specific conserved signature that has been detected in several previously studied *S. aureus* mRNAs (16). Moreover, as SprX_mutL3 does not influence the glycopeptide susceptibility (Figure 7B and C), the C-rich region of SprX is likely responsible for the regulation of other SprX targets involved in antibiotic resistance. This reinforces the notion that gene expression regulation by these sRNAs in *S. aureus* occurs through a shared mechanism. *In vitro*, SprX-mediated downregulation of SpoVG translation does not require any additional factors. This result is in agreement with previously reported *S. aureus* sRNAs that overcome the Hfq protein requirement for sRNA–mRNA duplex stabilization in enterobacteria (41).

The SprX-*yabJ-spoVG* mRNA interaction inhibits SpoVG translation initiation by preventing the binding of ribosomes to the *spoVG* RBS. The translation initiation inhibition is a strategy commonly used by bacterial sRNAs to control gene expression. sRNA pairing with mRNA targets can enhance or repress targeted gene translation (23,42,43). Generally, duplex formation between the mRNA target and sRNAs induces mRNA target degradation through the recruitment of bacterial ribonucleases (44). However, the strategy of translational inhibition without target mRNA degradation was shown to be sufficient to silence gene expression in both Gram-negative and -positive bacteria (28,45). Here, we show that SprX inhibits SpoVG translational initiation without inducing degradation of bicistronic *yabJ-spoVG* mRNA from which SpoVG is translated. Furthermore, the *yabJ-spoVG* mRNA is cleaved by an unknown mechanism into two separate transcripts that correspond to the *yabJ* and the *spoVG* mRNAs (8). Interestingly, SprX interacts with *yabJ-spoVG* mRNA in the region of the cleavage site (Figure 3A). We have shown that SprX does not affect the levels of full-length *yabJ-spoVG*; however, the overexpression of SprX decreases the *spoVG* and *yabJ* mRNAs levels (Figure 2C and D and Supplementary Figure S5B and C). This suggests that because SprX

interacts within the region of internal processing of *yabJ-spoVG* mRNA, its binding influence the mRNA cleavage. It has been shown that *yabJ-spoVG* mRNA cleavage occurs downstream from *spoVG* SD nucleotide sequence (9), which makes the translation of SpoVG impossible from *spoVG* transcript. Moreover, SpoVG is translated from full-length *yabJ-spoVG* mRNA (9). The physiological functions as well as the mechanism of the *yabJ-spoVG* mRNA processing remain to be identified, but this cleavage could serve to irreversibly inhibit *spoVG* expression.

Our results raised an important question concerning the combination of sRNA-mediated translational inhibition with mRNA degradation in *S. aureus*. mRNA–sRNA interactions can result in mRNA target degradations; therefore, gene silencing becomes irreversible, leading to the elimination of target mRNAs and sRNAs. In contrast, in the absence of sRNA-triggered mRNA degradation, mRNA target translation would rapidly resume once the sRNAs released target repression. Moreover, as SpoVG is translated from bicistronic *yabJ-spoVG* mRNA, sRNA-triggered operon mRNA degradation would also affect the expression of the operon's first protein, YabJ. We hypothesize that the strategy wherein SprX inhibits translation of SpoVG but without promotion of mRNA degradation, may allow for discoordinate gene expression in the *yabJ-spoVG* operon. Such a strategy of specific translational repression of a targeted gene within an operon while not modifying other operon gene expressions was described in *E. coli*, where Spot42 specifically inhibits *galK* of *galETKM* operon (45). We showed *in vitro* that SprX does not influence YabJ translation. Because the conditions of YabJ protein expression are not known (12), further studies will be necessary to investigate the conditions of YabJ expression *in vivo* and to show whether SprX sRNA is involved in its regulation *in vivo*.

In fact, sRNA-mediated operon control adds an additional layer to gene expression regulation. Diverse sRNA mechanisms for the adjustment of operon expression have been discovered. In addition to the aforementioned mechanism of specific translational inhibition of target operon genes, sRNA could also influence operon mRNA stability. sRNAs could trigger degradation of the entire operon mRNA (34), or of just a part of the operon, releasing a translationally active mRNA fragment (46). Furthermore, sRNA could also induce operon-mRNA cleavages (47). We presume that further studies on sRNA-mediated regulation of operon expression will help us to understand the complexity of their regulation, and will reveal new mechanisms of action.

Until now, sRNAs were described as being involved in the control of diverse cellular processes, including pathogenicity control. Two *S. aureus* regulatory sRNAs, SprD and Ssr42, have been shown to be essential for the virulence in an animal model of infection (28,29). An *S. aureus* paradigm for this emerging and expanding class of regulatory RNAs is RNAIII, the effector of the global *agr* regulon that controls the synthesis of multiple virulence factors (16,24–26). Moreover, a number of studies have linked alteration of the *agr* system function with Vancomycin tolerance [reviewed in (6)]. Although the mechanisms are not yet understood, the effect of *agr* on Vancomycin tolerance was proposed to be mediated by the expression of RNAIII (48). Recently, a case of antibiotic resistance regulation by a riboswitch was described (49). In that report, a riboswitch (a 5′ leader sequence within mRNA) was shown to control the translation of the mRNA-encoding aminoglycoside adenyl-transferase enzymes that confer resistance to aminoglycoside antibiotics. Drug binding to the mRNA leader releases the translation repression imposed by the riboswitch and induces bacterial resistance to aminoglycosides. Here, we report on a sRNA involved in bacterial resistance to antibiotics in a major human pathogen, *S. aureus*.

ACCESSION NUMBERS

NCTC8325 (accession no. NC_007795)

SpoVG NCTC8325 SAOUHSC_00469
GeneID:3920329

YabJ NCTC8325 SAOUHSC_00468
GeneID:3920328

RNAIII NCTC 8325 SAOUHSC_02260
GeneID:3919680
(Gene accession number: X52543)

SUPPLEMENTARY DATA

Supplementary Data are available at NAR Online.

ACKNOWLEDGEMENTS

We are grateful to Dr B. Berger-Bächi (Zurich, Switzerland) for the plasmid pSTM33 and the RN4220Δ*yabJ-spoVG* strain. We thank Dr M. Hallier and Y. Le Pétillon from the lab for the technical assistance and Pr. P.Y. Donnio (Rennes University) for helpful discussions and advices.

FUNDING

Institut National de la Santé et de la Recherche Médicale (INSERM), the Rennes University (Défis Scientifiques Emergents), the Région Bretagne ('allocation doctorale', PhD thesis) and the Fondation pour la Recherche Médicale [FRM; FDT20130928407 to A.E.]; Agence Nationale de la Recherche [ANR-09-MIEN-030-01 to B.F.]. Funding for open access charge: Inserm.

Conflict of interest statement. None declared.

REFERENCES

1. Grundmann,H., Aires-de-Sousa,M., Boyce,J. and Tiemersma,E. (2006) Emergence and resurgence of meticillin-resistant *Staphylococcus aureus* as a public-health threat. *Lancet*, **368**, 874–885.
2. Boger,D.L. (2001) Vancomycin, teicoplanin, and ramoplanin: synthetic and mechanistic studies. *Med. Res. Rev.*, **21**, 356–381.
3. Courvalin,P. (2006) Vancomycin resistance in gram-positive cocci. *Clin. Infect. Dis.*, **42(Suppl. 1)**, S25–S34.

4. Hiramatsu,K., Hanaki,H., Ino,T., Yabuta,K., Oguri,T. and Tenover,F.C. (1997) Methicillin-resistant *Staphylococcus aureus* clinical strain with reduced vancomycin susceptibility. *J. Antimicrob. Chemother*, **40**, 135–136.
5. Liu,C. and Chambers,H.F. (2003) *Staphylococcus aureus* with heterogeneous resistance to vancomycin: epidemiology, clinical significance, and critical assessment of diagnostic methods. *Antimicrob. Agents Chemother.*, **47**, 3040–3045.
6. Howden,B.P., Davies,J.K., Johnson,P.D., Stinear,T.P. and Grayson,M.L. (2010) Reduced vancomycin susceptibility in *Staphylococcus aureus*, including vancomycin-intermediate and heterogeneous vancomycin-intermediate strains: resistance mechanisms, laboratory detection, and clinical implications. *Clin. Microbiol. Rev.*, **23**, 99–139.
7. Renzoni,A., Andrey,D.O., Jousselin,A., Barras,C., Monod,A., Vaudaux,P., Lew,D. and Kelley,W.L. (2011) Whole genome sequencing and complete genetic analysis reveals novel pathways to glycopeptide resistance in *Staphylococcus aureus*. *PLoS One*, **6**, e21577.
8. Meier,S., Goerke,C., Wolz,C., Seidl,K., Homerova,D., Schulthess,B., Kormanec,J., Berger-Bachi,B. and Bischoff,M. (2007) sigmaB and the sigmaB-dependent arlRS and yabJ-spoVG loci affect capsule formation in *Staphylococcus aureus*. *Infect. Immun.*, **75**, 4562–4571.
9. Schulthess,B., Meier,S., Homerova,D., Goerke,C., Wolz,C., Kormanec,J., Berger-Bachi,B. and Bischoff,M. (2009) Functional characterization of the sigmaB-dependent yabJ-spoVG operon in *Staphylococcus aureus*: role in methicillin and glycopeptide resistance. *Antimicrob. Agents Chemother.*, **53**, 1832–1839.
10. Matsuno,K. and Sonenshein,A.L. (1999) Role of SpoVG in asymmetric septation in *Bacillus* subtilis. *J. Bacteriol.*, **181**, 3392–3401.
11. Jutras,B.L., Chenail,A.M., Rowland,C.L., Carroll,D., Miller,M.C., Bykowski,T. and Stevenson,B. (2013) Eubacterial SpoVG homologs constitute a new family of site-specific DNA-binding proteins. *PLoS One*, **8**, e66683.
12. Schulthess,B., Bloes,D.A., Francois,P., Girard,M., Schrenzel,J., Bischoff,M. and Berger-Bachi,B. (2011) The sigmaB-dependent yabJ-spoVG operon is involved in the regulation of extracellular nuclease, lipase, and protease expression in *Staphylococcus aureus*. *J. Bacteriol.*, **193**, 4954–4962.
13. Schulthess,B., Bloes,D.A. and Berger-Bachi,B. (2012) Opposing roles of sigmaB and sigmaB-controlled SpoVG in the global regulation of esxA in *Staphylococcus aureus*. *BMC Microbiol.*, **12**, 17.
14. Beisel,C.L. and Storz,G. (2010) Base pairing small RNAs and their roles in global regulatory networks. *FEMS Microbiol. Rev.*, **34**, 866–882.
15. Pichon,C. and Felden,B. (2005) Small RNA genes expressed from *Staphylococcus aureus* genomic and pathogenicity islands with specific expression among pathogenic strains. *Proc. Natl Acad. Sci. USA*, **102**, 14249–14254.
16. Geissmann,T., Chevalier,C., Cros,M.J., Boisset,S., Fechter,P., Noirot,C., Schrenzel,J., Francois,P., Vandenesch,F., Gaspin,C. *et al.* (2009) A search for small noncoding RNAs in *Staphylococcus aureus* reveals a conserved sequence motif for regulation. *Nucleic Acids Res.*, **37**, 7239–7257.
17. Marchais,A., Naville,M., Bohn,C., Bouloc,P. and Gautheret,D. (2009) Single-pass classification of all noncoding sequences in a bacterial genome using phylogenetic profiles. *Genome Res.*, **19**, 1084–1092.
18. Abu-Qatouseh,L.F., Chinni,S.V., Seggewiss,J., Proctor,R.A., Brosius,J., Rozhdestvensky,T.S., Peters,G., von Eiff,C. and Becker,K. (2010) Identification of differentially expressed small non-protein-coding RNAs in *Staphylococcus aureus* displaying both the normal and the small-colony variant phenotype. *J. Mol. Med.*, **88**, 565–575.
19. Beaume,M., Hernandez,D., Farinelli,L., Deluen,C., Linder,P., Gaspin,C., Romby,P., Schrenzel,J. and Francois,P. (2010) Cartography of methicillin-resistant *S. aureus* transcripts: detection, orientation and temporal expression during growth phase and stress conditions. *PLoS One*, **5**, e10725.
20. Bohn,C., Rigoulay,C., Chabelskaya,S., Sharma,C.M., Marchais,A., Skorski,P., Borezee-Durant,E., Barbet,R., Jacquet,E., Jacq,A. *et al.* (2010) Experimental discovery of small RNAs in *Staphylococcus aureus* reveals a riboregulator of central metabolism. *Nucleic Acids Res.*, **38**, 6620–6636.
21. Guillet,J., Hallier,M. and Felden,B. (2013) Emerging functions for the *Staphylococcus aureus* RNome. *PLoS Pathog.*, **9**, e1003767.
22. Tomasini,A., Francois,P., Howden,B.P., Fechter,P., Romby,P. and Caldelari,I. (2013) The importance of regulatory RNAs in *Staphylococcus aureus*. *Infect. Genet. Evol*, **21**, 616–626.
23. Waters,L.S. and Storz,G. (2009) Regulatory RNAs in bacteria. *Cell*, **136**, 615–628.
24. Morfeldt,E., Taylor,D., von Gabain,A. and Arvidson,S. (1995) Activation of alpha-toxin translation in *Staphylococcus aureus* by the trans-encoded antisense RNA, RNAIII. *EMBO J.*, **14**, 4569–4577.
25. Boisset,S., Geissmann,T., Huntzinger,E., Fechter,P., Bendridi,N., Possedko,M., Chevalier,C., Helfer,A.C., Benito,Y., Jacquier,A. *et al.* (2007) *Staphylococcus aureus* RNAIII coordinately represses the synthesis of virulence factors and the transcription regulator Rot by an antisense mechanism. *Genes Dev.*, **21**, 1353–1366.
26. Chevalier,C., Boisset,S., Romilly,C., Masquida,B., Fechter,P., Geissmann,T., Vandenesch,F. and Romby,P. (2010) *Staphylococcus aureus* RNAIII binds to two distant regions of coa mRNA to arrest translation and promote mRNA degradation. *PLoS Pathog.*, **6**, e1000809.
27. Novick,R.P., Ross,H.F., Projan,S.J., Kornblum,J., Kreiswirth,B. and Moghazeh,S. (1993) Synthesis of staphylococcal virulence factors is controlled by a regulatory RNA molecule. *EMBO J.*, **12**, 3967–3975.
28. Chabelskaya,S., Gaillot,O. and Felden,B. (2010) A *Staphylococcus aureus* small RNA is required for bacterial virulence and regulates the expression of an immune-evasion molecule. *PLoS Pathog.*, **6**, e1000927.
29. Morrison,J.M., Miller,E.W., Benson,M.A., Alonzo,F. III, Yoong,P., Torres,V.J., Hinrichs,S.H. and Dunman,P.M. (2012) Characterization of SSR42, a novel virulence factor regulatory RNA that contributes to the pathogenesis of a *Staphylococcus aureus* USA300 representative. *J. Bacteriol.*, **194**, 2924–2938.
30. Charpentier,E., Anton,A.I., Barry,P., Alfonso,B., Fang,Y. and Novick,R.P. (2004) Novel cassette-based shuttle vector system for gram-positive bacteria. *Appl. Environ. Microbiol.*, **70**, 6076–6085.
31. Herbert,S., Ziebandt,A.K., Ohlsen,K., Schafer,T., Hecker,M., Albrecht,D., Novick,R. and Gotz,F. (2010) Repair of global regulators in *Staphylococcus aureus* 8325 and comparative analysis with other clinical isolates. *Infect. Immun.*, **78**, 2877–2889.
32. Bruckner,R. (1997) Gene replacement in *Staphylococcus carnosus* and *Staphylococcus xylosus*. *FEMS Microbiol. Lett.*, **151**, 1–8.
33. Laemmli,U.K. (1970) Cleavage of structural proteins during the assembly of the head of bacteriophage T4. *Nature*, **227**, 680–685.
34. Antal,M., Bordeau,V., Douchin,V. and Felden,B. (2005) A small bacterial RNA regulates a putative ABC transporter. *J. Biol. Chem.*, **280**, 7901–7908.
35. Kuroda,M., Ohta,T., Uchiyama,I., Baba,T., Yuzawa,H., Kobayashi,I., Cui,L., Oguchi,A., Aoki,K., Nagai,Y. *et al.* (2001) Whole genome sequencing of meticillin-resistant *Staphylococcus aureus*. *Lancet*, **357**, 1225–1240.
36. Gillaspy,A.F., Worrell,V., Orvis,J., Roe,B.A., Dyer,D.W. and Iandolo,J.J. (2006) In: Fischetti,V., Ferretti,R.N.J., Portnoy,D. and Rood,J. (eds), *Gram-positive Pathogens*. ASM Press, Washington, DC, pp. 381–412.
37. Baba,T., Bae,T., Schneewind,O., Takeuchi,F. and Hiramatsu,K. (2008) Genome sequence of *Staphylococcus aureus* strain Newman and comparative analysis of staphylococcal genomes: polymorphism and evolution of two major pathogenicity islands. *J. Bacteriol.*, **190**, 300–310.
38. Tjaden,B. (2012) Computational identification of sRNA targets. *Methods Mol. Biol.*, **905**, 227–234.
39. Cao,Y., Wu,J., Liu,Q., Zhao,Y., Ying,X., Cha,L., Wang,L. and Li,W. (2010) sRNATarBase: a comprehensive database of bacterial sRNA targets verified by experiments. *RNA*, **16**, 2051–2057.
40. Papenfort,K. and Vogel,J. (2009) Multiple target regulation by small noncoding RNAs rewires gene expression at the post-transcriptional level. *Res. Microbiol.*, **160**, 278–287.

41. Jousselin,A., Metzinger,L. and Felden,B. (2009) On the facultative requirement of the bacterial RNA chaperone, Hfq. *Trends Microbiol.*, **17**, 399–405.
42. Frohlich,K.S. and Vogel,J. (2009) Activation of gene expression by small RNA. *Curr. Opin. Microbiol.*, **12**, 674–682.
43. Storz,G., Vogel,J. and Wassarman,K.M. (2011) Regulation by small RNAs in bacteria: expanding frontiers. *Mol. Cell*, **43**, 880–891.
44. Lalaouna,D., Simoneau-Roy,M., Lafontaine,D. and Masse,E. (2013) Regulatory RNAs and target mRNA decay in prokaryotes. *Biochim. Biophys. Acta*, **1829**, 742–747.
45. Moller,T., Franch,T., Udesen,C., Gerdes,K. and Valentin-Hansen,P. (2002) Spot 42 RNA mediates discoordinate expression of the *E. coli* galactose operon. *Genes Dev.*, **16**, 1696–1706.
46. Desnoyers,G., Morissette,A., Prevost,K. and Masse,E. (2009) Small RNA-induced differential degradation of the polycistronic mRNA iscRSUA. *EMBO J.*, **28**, 1551–1561.
47. Opdyke,J.A., Fozo,E.M., Hemm,M.R. and Storz,G. (2011) RNase III participates in GadY-dependent cleavage of the gadX-gadW mRNA. *J. Mol. Biol.*, **406**, 29–43.
48. Paulander,W., Nissen Varming,A., Baek,K.T., Haaber,J., Frees,D. and Ingmer,H. (2013) Antibiotic-mediated selection of quorum-sensing-negative *Staphylococcus aureus*. *MBio*, **3**, e00459–e00412.
49. Jia,X., Zhang,J., Sun,W., He,W., Jiang,H., Chen,D. and Murchie,A.I. (2013) Riboswitch control of aminoglycoside antibiotic resistance. *Cell*, **152**, 68–81.